Available online at www.sciencedirect.com
ScienceDirect
Journal of Bionic Engineering 13 (2016) 115–123

Sticking/Climbing Ability and Morphology Studies of the Toe Pads of Chinese Fire Belly Newt

Shuai Wang, Meng Li, Wei Huang, Xiaolei Wang

College of mechanical and electrical engineering, Nanjing University of Aeronautics and Astronautics, Nanjing 210016, *China*

Abstract

The Chinese fire belly newts (*Cynops orientalis*) have the ability to escape from the glass tank with vertical walls. An experimental device was developed to investigate the sticking and climbing behaviors of the newts. The detaching angles of the newt on the surfaces of glass, PMMA, and SUS 304 stainless steel at dry, little-water, and plenty-water conditions were measured and used as an index to evaluate the sticking and climbing abilities of the newts on tilted surface. The experimental results show that the newts have a strong ability to stick on tilted surface, particularly on the surface with little water. Morphological studies of the toe pads and belly were carried out by SEM and cryo-SEM to clarify the sticking mechanisms. It is found that the toe pad of the newt consists of a dense array of nanopillars with *ca* 100 nm – 300 nm diameter surrounded by small channels. This structure is supposed to facilitate high adhesion to substrate by providing capillary forces, and promote the squeeze-out of fluid between the toe pad and substrate in flooded case.

Keywords: newt, adhesion, climb, morphology, surface texture

doi: 10.1016/S1672-6529(14)60165-7

1 Introduction

Nature provides many appealing and enigmatic surfaces, which are of great significance for the biomimetic designing process of various interfaces in human life[1–6]. The discovery of the micro- and nano-structures on lotus leaf surface offers an idea to manufacture super-hydrophobic and self-cleaning surfaces. The understanding on the mechanisms of the longitudinal ribs on shark skin inspires people to design the swimming wear and the surface of flap with reduced drag force[7].

The surfaces facilitating strong adhesion associated with high friction have received a significant boost in the last decade not only on the phenomena and mechanisms[8], but also on the biomimetic manufacturing technology[9,10]. The carnivorous plant *Roridula gorgonias* can secrete a viscous resinous. Their glandular trichomes still possess the capacity to adhere to glass surfaces either hydrophilic or hydrophobic even after being submersed in water for one day[11]. Attaching ability is also the survival foundation of small animals in their complex environments. Some insects can produce adhesive forces equivalent to more than 100 times their own body weight on perfectly smooth surfaces[12].

There are various actions including hooks, lock, suction, dry or wet adhesion between the toe pads of animals and substrate[13]. The flies and beetles mainly use their tenent setae terminally covered with pad secretion to attach the smooth surface[14–18], and the similar structures are also found on spiders feet[19–21]. Geckos are exceptional in their ability to climb rapidly up a dry and smooth vertical surface. Microscopy has shown that a gecko's foot has nearly five hundred thousand keratinous hairs or setae. Each seta is 30 μm – 130 μm long and contains hundreds of projections terminating in 0.2 μm – 0.5 μm spatula-shaped structures, supporting the hypothesis that gecko's foot operate by van der Waals forces[22,23].

Tree frogs have a remarkable ability to cling to the wet smooth surface utilizing their toe pads, which are soft and patterned with a regular hexagonal microstructure of approximately 10 μm epidermal cells indiameter separated by approximately 1 μm channels in

Corresponding author: Xiaolei Wang
E-mail: wxl@nuaa.edu.cn

wideth[24–28]. Suction[29,30] and glue-like function[31] were assumed as the attaching mechanisms in the early studies, but those have been disputed later. The accepted explanations include: the bending elasticity of the toe pad on distances larger than the size of the blocks is reduced by the channels, resulting in the increase in toe-pad-substrate contact area; the mucus stored in the channels generates a relative long-range attractive interaction due to the formation of capillary bridges; and on the surfaces wetted by rain, the channels may act to disperse excess fluid to the pad edge to form the direct contact between the toe pad and substrate[32]. Additionally, Federle *et al*. presented that the remarkable attachment of tree frogs was not solely contributed by the wet adhesive force, but also the boundary friction on the microstructures of the pad epidermis[33]. Similar structures have also been found in torrent-living ranid frogs and bush crickets[34–36]. Preliminary studies demonstrated that the toe pads of *Amolops spp*. had distinct anatomical differences from the typical pattern found in tree frogs. The toe pad epithelial cells were elongated providing much straighter channels between the centre of the pad and the periphery. An obvious function for these shorter pathways from centre to edge of pad would promote rapid drainage of excess fluid from underneath the pad. Those instances bear ample testimony to the biodiversity. Although the evolution demonstrates a convergent process, species evolve a variety of micro-structures with large or small differences to adapt to the different ecosystems.

The Chinese fire belly newt is a genus of newts native to China, commonly seen in pet stores. Recently, we found that the newt has the ability to escape from a glass tank with vertical walls, which raise the questions that how does newt get the adhesive and climbing properties and what is the structure on its toe pads? Because the newts move in the way of crawling, to clarify the structure and mechanisms of its toe pads has the potential for the development of new adhesive surfaces, such as the leg of the endoscopic capsule, which is required to work under wet conditions.

In this paper, the sticking and climbing properties of the Chinese fire belly newt were evaluated on three different surfaces under dry and wet conditions. The toe pad morphology and venter skin were explored by SEM and cryo-SEM. The relationship between the morphology of the toe pads and sticking/climbing properties was discussed.

2 Materials and methods

2.1 Animals

The Chinese fire belly newt is a genus (*Cynops orientalis*) of newts native to China. It is an semiaquatic amphibian of the family Salamandridae. As shown in Fig. 1, in appearance, the Chinese fire belly newt has a head like a lizard, four feet, and four toes on forelimb, five toes on hindlimb. It is a small newt usually with the length of 5 cm –10 cm, has black back and bright-orange aposematic coloration on its belly. The Chinese fire belly newts are mildly poisonous and excrete toxins through their skin.

The newts used in this study have the length range from 5 cm to 7 cm, and weight range from 1.0 g to 3.0 g. As an amphibian and reptile, the crawling action of the Chinese fire belly newt is the same to other reptile, as shown in Fig. 2.

2.2 Sticking and climbing experiments

A simple device as shown in Fig. 3 has been developed to evaluate the sticking and climbing abilities of the newt. A frame assembled with the testing surface is fixed to the base via an axle. By pulling the wire tied to the frame, the frame could rotate smoothly around the axle to tilt the testing surface from 0˚ to 180˚.

(a) (b)

Fig. 1 The Chinese fire belly newt; (a) the back side view; (b) the belly side view.

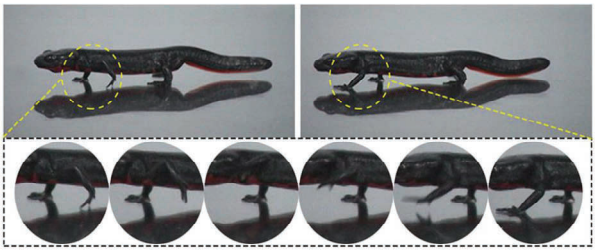

Fig. 2 The crawling mode of the Chinese fire belly newt.

A protractor is settled at the axle to measure the inclined angle of the testing surface. The testing surface in the frame is replaceable, with the dimensions of 210 mm ×160 mm.

Glass, PMMA(Polymethylmethacrylate) and SUS 304 stainless steel with relative smooth or rough surfaces are used. Most of the materials are obtained from market, and the original surfaces are directly used in the experiments. The rough surfaces of glass and SUS 304 steel are achieved by abrasive jet machining with SiC particles of 15 μm in diameter. Table 1 lists the surface roughness and water contact angles of the testing surfaces.

Before the experiments, the testing surface was cleaned by ethanol, deionized water, and dried by nitrogen in sequence. Then, water was sprayed on the surface to create two wet conditions. "Little-water" is the case that there are only small and dense water drops sprayed on the surface. "Plenty-water" is that the water drops have connected and spread on the surface by more water sprayed. Figs. 3b, 3c and 3d show the images of the dry, little-water, and plenty-water conditions on a rough SUS 304 stainless steel surface, respectively. While testing, the newt was taken from the containing box, blotted by filter paper to remove the water on its body, and then placed on the testing surface appropriately. By pulling the wire slowly to tilt the testing surface, the newt would begin to slid or drop off the surface at a certain angle, which was defined as the detaching angle, and recorded to evaluate the sticking and climbing abilities of the newt.

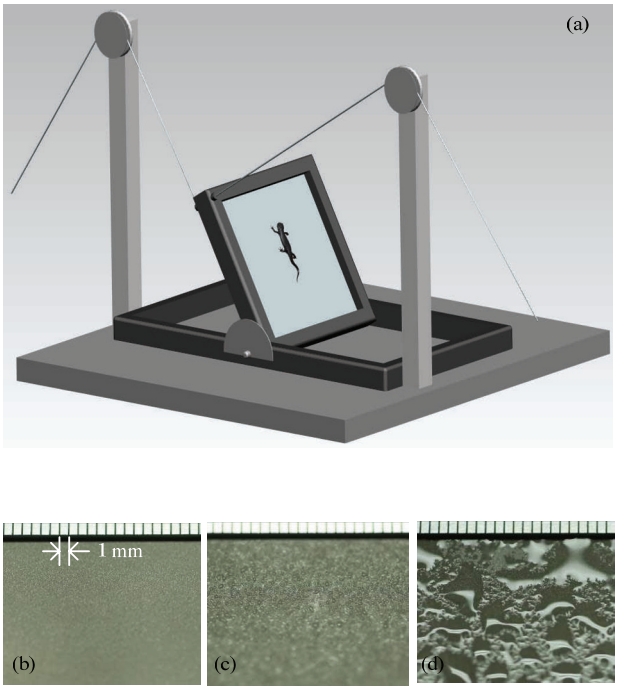

Fig. 3 (a) Schematic diagram of the experimental device; images of (b) dry, (c) little-water and (d) plenty-water conditions on a rough SUS 304 stainless steel surface.

Table 1 The surface roughness and water contact angles of testing surfaces

Materials	Surfaces	Roughness (Ra, μm)	Contact angle (˚)
Glass	Smooth	0.008	35±5
	Rough	2.510	65±6
PMMA	Smooth	0.004	70±5
	Rough	3.160	93±2
SUS 304	Smooth	0.020	79±4
	Rough	1.420	64±2

2.3 Sample preparation for SEM

The toe pad and belly skin of the newt were cut off by medical scalpel and rinsed in normal saline to remove the residual stain on the surface. Then, the samples were fixed in 2.5% glutaraldehyde for 2 h at 4 ˚C and rinsed in 0.1 M phosphate buffer for three times (15 min per rinse). Next, the samples were dehydrated through an ethanol series (50%, 70%, 80%, 90%, 95% and 100%, 15 min each) in sequence, and were placed in an automatic critical point dryer (Leica EM CPD300, Leica Microsystems, Wetzlar, Germany) to get a completely dry state. The dried sample was attached on the sample stage using double side adhesive tape and coated with gold approximately 10 nm in thickness by a vacuum sputter coater (SCD500 Sputter, Pfäffikon ZH, Switzerland). Finally, the prepared samples were observed by S-4800 SEM (Hitachi Ltd, Tokyo, Japan).

2.4 Sample preparation for cryo-SEM

The procedure of cryo-SEM can avoid the formation of ice crystals and prevent damages to the structure of bio-materials. The same as above, the belly skin was cut off by medical scalpel and washed up by normal saline. After blotting up the water on the skin surface, the sample was fixed on an appropriate holder and plunged into liquid nitrogen. Then, the sample was placed on the cool stage of SEM, put into the preparation chamber, and transferred into the observation chamber in sequence when the vacuum degree meets the requirements. Finally, the sample was examined using S-4800 SEM (Hitachi Ltd, Tokyo, Japan).

3 Results and Discussion

3.1 Sticking and climbing experiments

3.1.1 Sticking experiments on different surfaces

The sticking ability of the newts on the surfaces of glass, PMMA, and SUS 304 stainless steel with different surface roughness (smooth and rough) were evaluated under different wet conditions (dry, little-water, and plenty-water). Three different newts were used, and tested for five times for each. The vertical axis in Figs. 4, 5, and 6 represents the detaching angles of the newt on the different testing surfaces.

Fig. 4 shows the results on the glass surfaces. At little-water condition, there is not much difference on the smooth and the rough surfaces. In both cases, the detaching angle could be as high as 180˚, demonstrating the best sticking ability compared to the cases of dry and plenty-water conditions. At the dry condition, the detaching angles on both smooth and rough surfaces were obviously lower than that in the case of little-water. With plenty water on the smooth surface, the detaching angle decreased to around 90˚, much lower than that at dry and little-water conditions, showing the slippery phenomenon. On the rough surface with plenty water, the detaching angle varied in a wide range from 90˚ to 180˚, showing the newts might stick on the surface and might detach at the angle around 90˚. This might because of the complexity of the surface combined with the uniformity of water and surface roughness.

Fig. 5 shows the sticking ability of the newts on the PMMA surfaces. The overall performance was similar to that on the glass surface. At dry condition on the smooth surface, the detaching angles were as high as that at the condition of little-water condition, and higher than that on the glass surface.

Fig. 6 shows the sticking ability of the newts on the surfaces of SUS 304 stainless steel. At the plenty-water condition, the detaching angles varied and were very low on the smooth surface, showing a slippery phenomenon. At the dry condition, the detaching angles could be as high as that at little-water condition, and could be lower than that at little-water condition. Similar to the glass and PMMA surfaces, the detaching angles of the newts shows relative high and stable value at little-water condition. The similarity of the sticking ability at little water condition on the three different surfaces might indicate that the toe pads of the newt could be suitable for various surfaces in the nature.

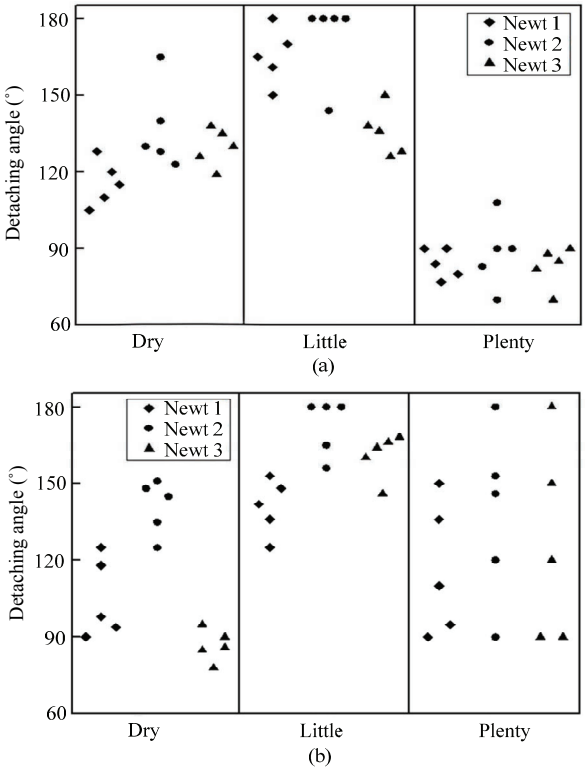

Fig. 4 The sticking ability of the newts on glass surfaces: (a) Smooth surface; (b) rough surface.

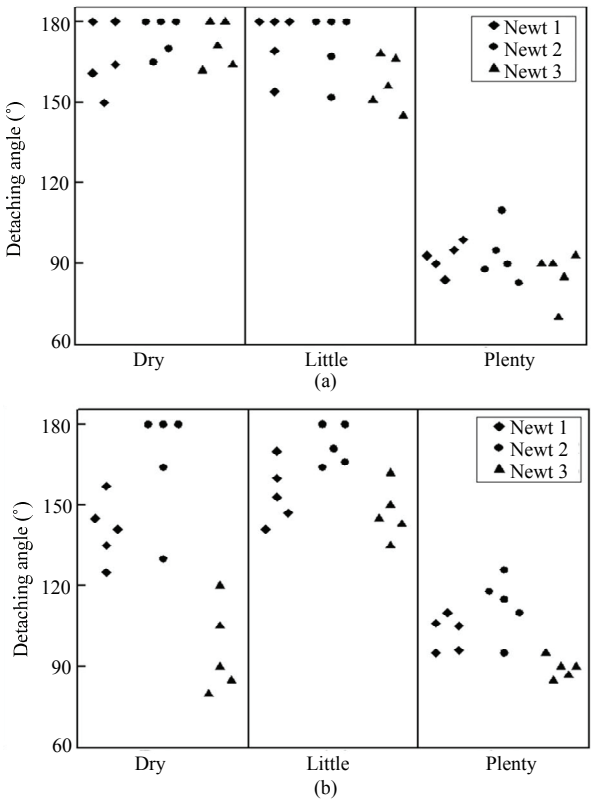

Fig. 5 The sticking ability of the newts on PMMA surfaces: (a) Smooth surface; (b) rough surface.

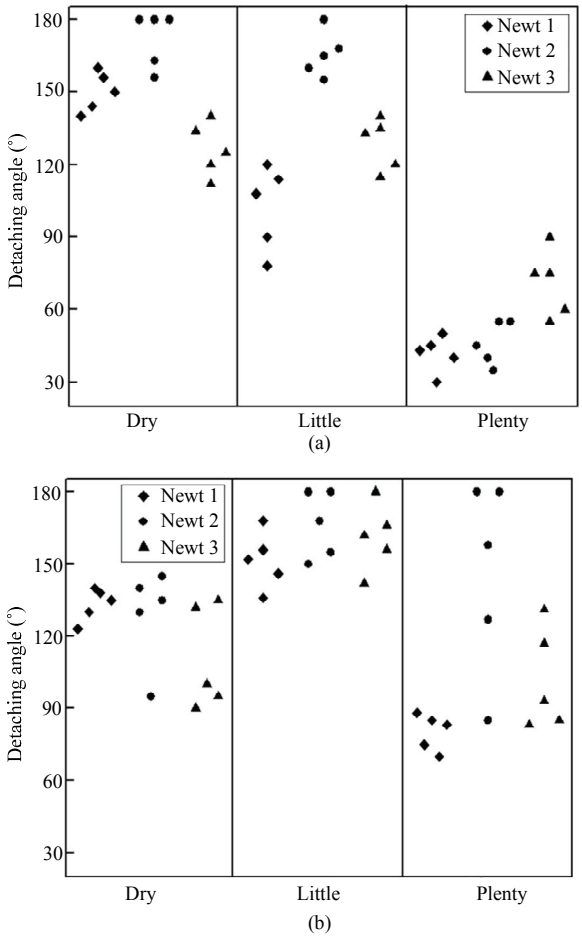

Fig. 6 The sticking ability of the newts on the surface of SUS 304 stainless steel: (a) Smooth surface; (b) rough surface.

3.1.2 Climbing experiments on different surfaces

While the newt is sticking on the surface tilted with a large angle, not only the four feet, but also the belly and tail could attach to the surface, which is supposed to improve its sticking ability. However, there is no contact between its body and the surface while the newt crawls. Furthermore, its one foot needs to detach the surface in order to move forward as shown in Fig. 2. Hence, climbing is much more difficult than sticking on a tilted surface without moving.

Because the newts are easy to get slipped at plenty-water condition, the climbing tests were only carried out at dry and little-water conditions. Fig. 7 shows the maximum tilt angle that the newt could stay and climb on the surface. It is found that the maximal climbing angle is in the range from 30˚ to 80˚, much lower than the detaching angles shown in Figs. 4, 5 and 6. On those three surfaces, it is interesting that the newt has a greater climbing ability on the smooth surface than the rough one at dry condition. However, it is opposite at little-water condition.

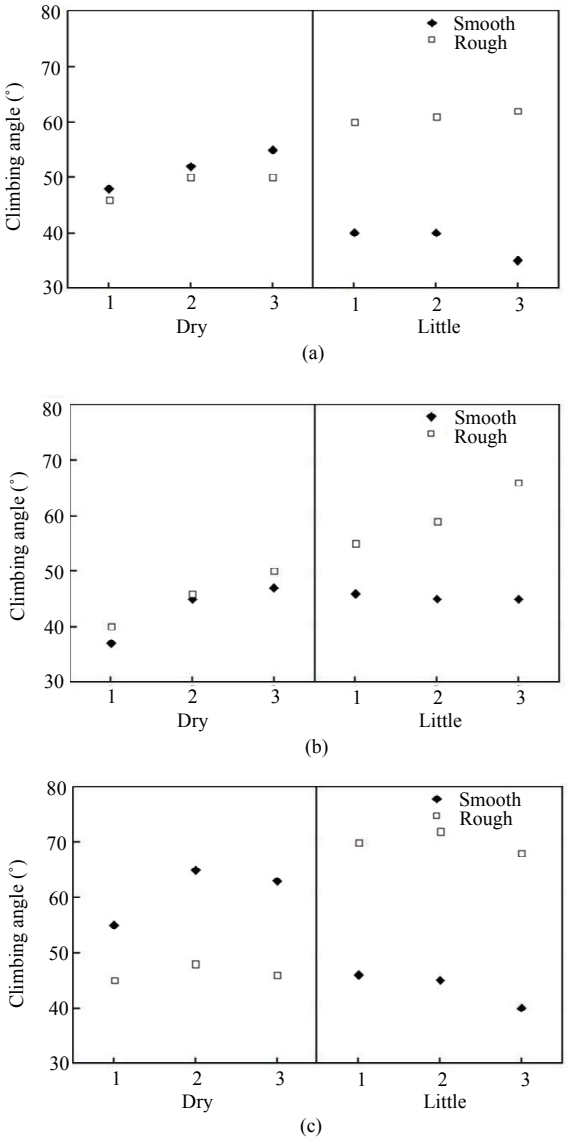

Fig. 7 Climbing ability of the newt on three different surfaces: (a) Glass; (b) PMMA; (c) SUS 304 stainless steel.

3.2 Skin morphology of newt

The above experiment results clearly show the sticking and climbing abilities of the newts on tilted surfaces under different conditions. In order to clarify the mechanisms of adhesion, morphological studies were carried out on the toe pads and belly skin.

3.2.1 Toe pads morphology

Similar to the tree frog, the newt has four toes in each forelimb and five in hindlimb as shown in Fig. 1. However, unlike the toe pads of the tree frog, which are

located on the expanded tips of each toe, the shape of the toes of the newt looks like the finger of human beings in the SEM image shown in Fig. 8a. The attaching mode of the newt is also different from that of tree frogs. The newts use both the toes and thenar to stick on the surface. To enlarge the area on the toe, as shown in Fig. 8b, it is found that the toe surface consists of polygonal epithelial cells of *ca* 20 μm – 30 μm in diameter separated by a border with a width of *ca* 200 nm between cells. The border between the cells in Fig. 8b seems to be a narrow networking groove, but it is different from that of tree frogs. On each epithelial cell, there is a dense array of hemispheric bulges or nanopillars with *ca* 100 nm – 300 nm diameter surrounded by small channels as shown in Fig. 8c.

Fig. 9 shows the structure of mucus gland, which lies among the epithelial cells on both toe and belly skin. The shape appears as circle or ellipse, which might be due to the deformation during sample preparation. Fig. 9c shows the details of a mucus gland. The mucus gland is made up by several cells around and its size just exceeds 10 μm. The inner wall of the mucus gland is visible, where the nano-structures are as same as the outside. The black arrows indicate the cell edges. In the SEM image, the mucus is not visible.

3.2.2 Belly skin morphology

Thinner and softer than the foot, the belly skin preparation for SEM was more difficult than that of the foot. The skin was easy collapsed compared to the toe pad. In Fig. 10a, the wrinkle pointed by arrow is along the widthways of the belly. Similar to the palm print on the human skin, many wrinkles lie on the belly both in the directions of widthways and lengthways, particularly, in lengthways, which may be the results of bending process. As shown in Fig. 10b, the epithelial cells are still visible. They are in the shape of irregular polygon connected to each other. The border between cells looks as the same as that on toe pads. However, it is interesting that the nano-structure on a single epithelial cell consists of numerous ostioles, contrary to the hemispheric bulges on the epithelial cell of toe pad. The mucus gland can still be found on the belly. As shown in Fig. 11a, it is clear that the holes formed by several cells connect together. Figs. 11b and 11c show the gland structure observed by the cryo-SEM. The images seem that there is something covering the skin and filling in the ostioles. It could be the mucus remained by the procedure of cryo-SEM. By comparing Fig. 10c and Fig. 11b, it is found that the nano-ostioles in cryo-SEM image are a little bit larger than that of SEM at the same

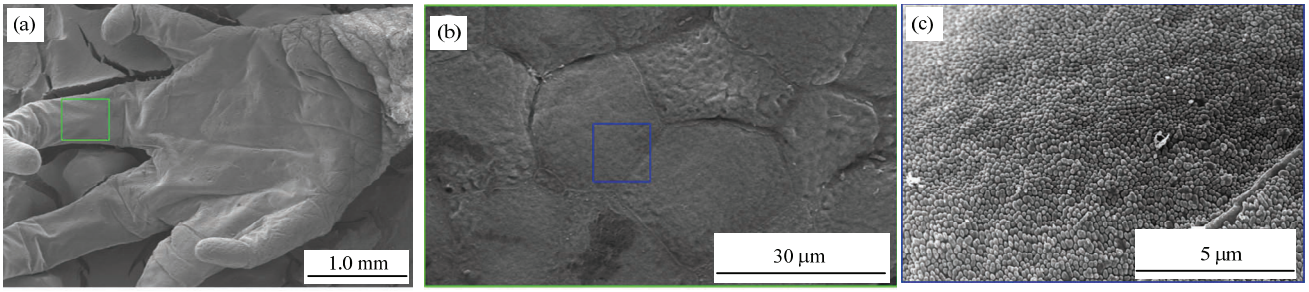

Fig. 8 Progressively enlarged views on the toe of the Chinese fire belly newt: (a) SEM image of the toe; (b) enlarged SEM image of the green square in (a); (c) enlareged SEM image of the blue square in (b).

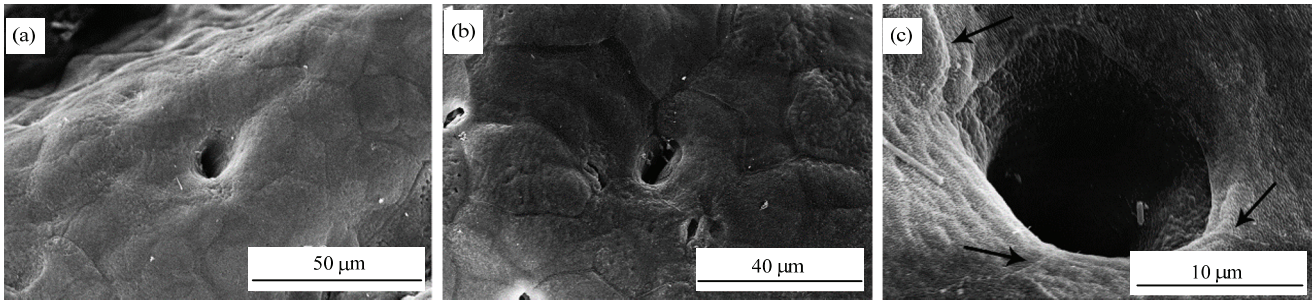

Fig. 9 The mucus gland: (a) On the toe; (b) on the belly; (c) enlarged image.

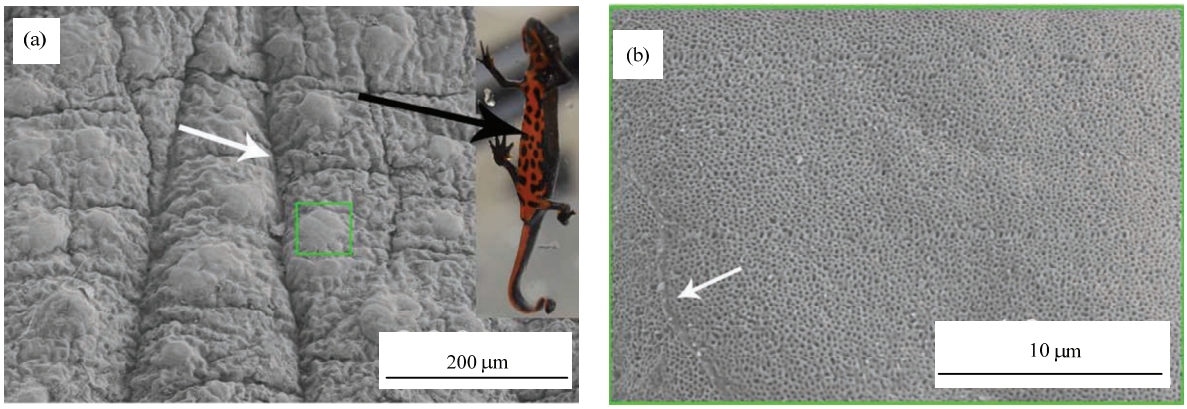

Fig. 10 (a) SEM image of the belly skin of the Chinese fire belly newt, (b) enlarged SEM image of the green square in (a).

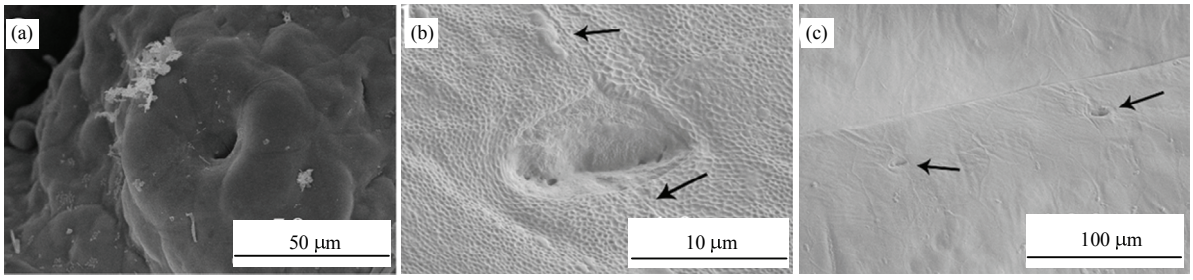

Fig. 11 (a) SEM image of mucus gland on the belly of the newt, (b) cryo-SEM image of mucus gland, (c) cryo-SEM image of two adjacent mucous glands.

magnification. The reason is that the process of sample preparation for SEM makes the sample slightly shrink[37,38].

3.3 Sticking function and the mechanisms

Surface waviness and roughness are the main reasons why macroscopic solids usually do not adhere to each other. On the other hand, in nature world, strong adhesion is possible even to very rough and curved surfaces by using non-compact solid structures consisting of either fiber-plate array structures or foam-like structures[32]. The toe pad of the newt consists of polygonal epithelial cells separated by the borders. Although there are no deep channels like that of tree frog, the toe pad with this structure is supposed to be bended easily to provide a firm grip on curved surface. In our previous study, it is also proven that such polygon or hexagon pattern could increase the toe-pad-substrate contact area, which will result in high dynamic friction as well as boundary friction between contacting surfaces[39], and the peg-studded hexagonal patterns are favorable for keeping the surface moist to produce a high friction force[40]. However, since there are no deep channels filled with mucus like that of tree frog, the polygonal epithelial cells in micro-meter scale on the toe pad of the newt might not be the leading structure of adhesion as that of the tree frog.

Although the top of epithelial cells of the tree frog is covered by a dense array of peg-like projections, there is no enough discussion on their functions so far. The nanostructure of the toe pads of the newt has distinct shape differences from the typical pattern seen in tree frogs. The nanopillars might play an important role in the adhesion process. As shown in Fig. 8c, on each epithelial cell there are dense nanopillars with hemispheric head of *ca* 100 nm – 300 nm diameter surrounded by small channels. The capillary force and drainage ability of flooded water might be facilitated by this structure. Otherwise, there is no proposed explanation that could be applied for the adhesive mechanism of the newts.

The adhesive and crawling ability of newts are mainly determined by the structures on its toe pad. The dense nanopillars seem to be easy deformed to create a large contact area with substrate, so that there is no obvious difference of adhesive properties on a smooth

surface and a rough surface in most cases shown in Figs. 4, 5 and 6. Because the channels between the nanopillars are smaller in size than that between the epithelial cells of tree frog, the drainage ability of newt toe pad might not be as high as that of the tree frog, so that the adhesive ability of newt on the surface with plenty-water is not as high as that on the surfaces of dry and little-water conditions.

The newt is a semiaquatic amphibian. Although the structure like mucus gland was observed on its toe and belly, and mucus like material was found by cryo-SEM as shown in Fig. 11, obviously, the effect of mucus is not as obvious as the tree frog. The adhesive ability usually is higher on the surface with little water than that on a dry surface, indicating that a little water might help to facilitate fast adhesion to substrate by capillary forces.

It is observed that the newt could have a high detaching angle while it has its belly and tail attached on the surface. The mucus gland is also found on the belly. However, the structure on belly skin is the array of dimples instead of nanopillars on the toe pad. Except for excreting toxins through their skin, the function of the structure on the belly skin is still unknown and further study is needed.

4 Conclusion

In this paper, a series of experiments were carried out to evaluate the sticking and climbing abilities of the newt on the surfaces of glass, PMMA, and SUS 304 stainless steel under different wet conditions. The toe pad morphology and belly skin were observed via SEM and cryo-SEM.

In most cases on either smooth or rough surface, the newts could stick on the surface tilted with the angle larger than 90° while the surface is dry or with little water, and it seems that the sticking ability is little greater at little-water condition than that at dry condition. At plenty water condition, varied experimental data show a slippery phenomenon in some cases.

The toe pad of the newt shows a distinct feature that is different from that of the tree frog. It consists of polygonal epithelial cells of *ca* 20 μm – 30 μm diameter separated by a border. On each epithelial cell there is a dense array of nanopillars with *ca* 100 nm – 300 nm diameter surrounded by small channels. This nanostructure is supposed to be the major structure, which facilitate fast adhesion to substrate by capillary forces, and act to squeeze-out the fluid between the toe pad and the substrate on flooded surface.

Acknowledgment

This research was supported by the National Nature Science Foundation of China (NSFC) (No. 51175246).

References

[1] Evans C J, Bryan J B. "Structured", "textured" or "engineered" surfaces. *Annals of the CIRP*, 1999, **48**, 541–556.

[2] Ren L, Han Z, Li J, Tong J. Effects of non-smooth characteristics on bionic bulldozer blades in resistance reduction against soil. *Journal of Terramechanics*, 2002, **39**, 221–230.

[3] Ren L. Progress in the bionic study on anti-adhesion and resistance reduction of terrain machines. *Science in China Series E*: *Technological Sciences*, 2009, **52**, 273–284.

[4] Huang W, Jiang L, Zhou C, Wang X. The lubricant retaining effect of micro-dimples on the sliding surface of PDMS. *Tribology International*, 2012, **52**, 87–93.

[5] Yu H, Huang W, Wang X. Dimple patterns design for different circumstances. *Lubrication Science*, 2013, **25**, 67–78.

[6] Niu S, Li B, Mu Z, Yang M, Zhang J, Han Z, Ren L. Excellent structure-based multifunction of morpho butterfly wings: A review. *Journal of Bionic Engineering*, 2015, **12**, 170–189.

[7] Bechert D W, Bruse M, Hage W, Meyer R. Fluid mechanics of biological surfaces and their technological application. *Naturwissenschaften*, 2000, **87**, 157–171.

[8] Bhushan B. Biomimetics: Lessons from nature-an overview. *Philosophical Transactions of the Royal Society A*, 2009, **367**, 1445–1486.

[9] Cohen D, Kligerman Y, Etsion I. The Effect of surface roughness on static friction and junction growth of an elastic-plastic spherical contact. *Journal of Tribology*, 2009, **131**, 021404.

[10] He Q, Yu M, Li Y, Chen X, Zhang H, Gong L, Dai Z. Adhesion Characteristics of a novel synthetic polydimethylsiloxane for bionic adhesive pads. *Journal of Bionic Engineering*, 2014, **11**, 371–377.

[11] Voigt D, Konrad W, Gorb S. A universal glue: Underwater adhesion of the secretion of the carnivorous flypaper plant Roridula gorgonias. *Interface Focus*, 2015, **5**, 20140053.

[12] Federle W, Brainerd E L, McMahon T A, Holldobler B. Biomechanics of the movable pretarsal adhesive organ in ants and bees. *Proceedings of the National Academy of Sciences of the United States of America*, 2001, **98**, 6215–6220.

[13] Gorb S N. Biological and biologically inspired attachment

systems, in Bhushan B (ed), *Handbook of Nano-technology*, Springer, Germany, 2010, 1525–1545.

[14] Langer M G, Ruppersberg J P, Gorb S. Adhesion forces measured at the level of a terminal plate of the fly's seta. *Proceedings of the Royal Society B*, 2004, **271**, 2209–2215.

[15] Eisner T, Aneshansley D J. Defense by foot adhesion in a beetle (*Hemisphaerota cyanea*). *Proceedings of the National Academy of Sciences of the United States of America*, 2000, **97**, 6568–6573.

[16] Bullock J M, Drechsler P, Federle W. Comparison of smooth and hairy attachment pads in insects: Friction, adhesion and mechanisms for direction-dependence. *Journal of Experimental Biology*, 2008, **211**, 3333–3343.

[17] Dirks J H. Physical principles of fluid-mediated insect attachment-Shouldn't insects slip? *Beilstein Journal of Nanotechnology*, 2014, **5**, 1160–1166.

[18] Niederegger S, Gorb S, Jiao Y. Contact behaviour of tenent setae in attachment pads of the blowfly *Calliphora vicina* (Diptera, Calliphoridae). *Journal of Comparative Physiology A*: *Sensory*, *Neural*, *and Behavioral Physiology*, 2002, **187**, 961–970.

[19] Kesel A B. Adhesion measurements on the attachment devices of the jumping spider *Evarcha arcuata*. *Journal of Experimental Biology*, 2003, **206**, 2733–2738.

[20] Kesel A B, Martin A, Seidl T. Getting a grip on spider attachment: An AFM approach to microstructure adhesion in arthropods. *Smart Materials and Structures*, 2004, **13**, 512.

[21] Niederegger S, Gorb S. Friction and adhesion in the tarsal and metatarsal scopulae of spiders. *Journal of Comparative Physiology A*, 2006, **192**, 1223–1232.

[22] Autumn K, Liang Y A, Hsieh S T, Zesch W, Chan W P, Kenny T W, Fearing R, Full R J. Adhesive force of a single gecko foot-hair. *Nature*, 2000, **405**, 681–685.

[23] Filippov A E, Gorb S N. Spatial model of the gecko foot hair: Functional significance of highly specialized non-uniform geometry. *Interface Focus*, 2015, **5**, 20140065.

[24] Welsch U, Storch V, Fuchs W. The fine structure of the digital pads of rhacophorid tree frogs. *Cell and tissue research*, 1974, **148**, 407–416.

[25] Green D M. Treefrog toe pads: Comparative surface morphology using scanning electron microscopy. *Canadian Journal of Zoology*, 1979, **57**, 2033-2046.

[26] Ernst V V. The digital pads of the tree frog, *Hyla cinerea*. II. the mucous glands. *Tissue and Cell*, 1973, 5, 97–104.

[27] Green D M, Simon M P. Digital microstructure in ecologically diverse sympatric microhylid frogs, genera cophixalus and sphenophryne (amphibia, Anura), from Papua-new-Guinea. *Australian journal of zoology*, 1986, **34**, 135–145.

[28] Ernst V V. The digital pads of the tree frog, *Hyla cinerea*. I. the epidermis. *Tissue and Cell*, 1973, 5, 83–96.

[29] Peters J A. *Dictionary of Herpetology*, Hafner Publ. Co., New York, 1964,

[30] Porter K R. *Herpetology*, Saunders W B. Co., Philadelphia, 1972.

[31] Dewitz H. Ueber die Fortbewegung der Thiere an senkrechten, glatten Flächen vermittelst eines Secretes. *Pflügers Archiv European Journal of Physiology*, 1884, **33**, 440–481. (in German)

[32] Persson B N J. Wet adhesion with application to tree frog adhesive toe pads and tires. *Journal of Physics*: *Condensed Matter*, 2007, **19**, 376110.

[33] Federle W, Barnes W J, Baumgartner W, Drechsler P, Smith J M. Wet but not slippery: Boundary friction in tree frog adhesive toe pads. *Journal of the Royal Society Interface*, 2006, **3**, 689–697.

[34] Barnes W J P. Functional morphology and design constraints of smooth adhesive pads. *MRS bulletin*, 2007, **32**, 479–485.

[35] Drotlef D M, Appel E, Peisker H, Dening K, del Campo A, Gorb S N, Barnes W J P. Morphological studies of the toe pads of the rock frog, Staurois parvus (family: Ranidae) and their relevance to the development of new biomimetically inspired reversible adhesives. *Interface Focus*, 2014, **5**, 20140036.

[36] Gorb S N, Jiao Y, Scherge M. Ultrastructural architecture and mechanical properties of attachment pads in *Tettigonia viridissima* (Orthoptera Tettigoniidae). *Journal of Comparative Physiology A*, 2000, **186**, 821–831.

[37] Rui Y, Lingna Z, Jingwei F, Jianli W, Kefeng F, Tongquan Y, Shaohui W, Yanli D. Insect specimens for scanning electron microscopy. *Journal of Beijing University of Agriculture*, 2014, **29**, 33–35. (in Chinese)

[38] Su-zhi G, Qing-e J. Drying methods of insect specimens for scanning electron microscopy. *Journal of Fujian Agricultural University*, 2001, **30**, 262–265.

[39] Huang W, Wang X. Biomimetic design of elastomer surface pattern for friction control under wet conditions. *Bioinspiration & Biomimetics*, 2013, **8**, 046001.

[40] Li M, Huang W, Wang X. Bioinspired, peg-studded hexagonal patterns for wetting and friction. Biointerphases, 2015, **10**, 031008.